DOI: https://doi.org/10.37434/tpwj2025.08.05

MODEL OF THE ANODE BOUNDARY LAYER IN WELDING ARCS

I.V. Krivtsun[1], A.I. Momot[1,2], I.B. Denysenko[1,3], U. Reisgen[4], O. Mokrov[4], R. Sharma[4]

[1]E.O. Paton Electric Welding Institute of the NASU
11 Kazymyr Malevych Str., 03150, Kyiv, Ukraine,
[2]Taras Shevchenko National University of Kyiv
64/13 Volodymyrs'ka Str., 01601, Kyiv, Ukraine,
[3]V.N. Karazin Kharkiv National University
4 Svobody Sq., 61022, Kharkiv, Ukraine
[4]Welding and Joining Institute, RWTH Aachen University
49 Pontstrasse, 52062, Germany

ABSTRACT

A one-dimensional model of the anode boundary layer in atmospheric pressure electric arcs with refractory cathode and evaporating anode is proposed for two modes of the anode metal evaporation: diffusive and convective. The corresponding systems of differential and algebraic equations are formulated to compute the spatial distributions of the number densities and diffusive flux densities of electrons, ions, and atoms; the electron temperature and the heavy particle (atoms and ions) temperature; and the electric potential in the plasma of the anode layer. Additionally, the model allows to calculate the heat flux introduced by the arc into the anode. The boundary conditions for the differential equations of this model at the boundaries of the anode layer with the arc column plasma and the space-charge sheath are formulated. An approach for determining the plasma parameters at these boundaries is also proposed for each evaporation mode.

KEYWORDS: anode boundary layer, welding arc, modelling, evaporating anode, metal vapor, diffusive evaporation, convective evaporation

INTRODUCTION

An important feature of welding arcs is the multi-component nature of arc plasma, which is associated with the presence, along with shielding gas particles, of the atoms and ions of metal vapor entering the arc due to evaporation of electrode material or the metal being welded [1–3]. Under TIG/PTA, and hybrid (TIG/PTA + laser) welding conditions, the main source of vapor in the arc is the metal being welded (anode of the arc) [4–6], since evaporation of the material of a refractory cathode operating in a thermionic mode is negligible.

At the same time, even a small amount of evaporated anode metal in the arc plasma of inert (shielding/plasma-forming) gas significantly affects its ionization composition, thermodynamic, transport, and optical properties. This leads to significant changes in thermal, electrical and gas-dynamic characteristics of the arc column plasma and of the anode boundary layer during TIG welding compared to the atmospheric pressure arc discharge with refractory (tungsten) cathode and non-evaporating, e.g. water-cooled anode [7–8].

In TIG/PTA, and hybrid (TIG/PTA + laser) welding, the temperature on the weld pool surface changes in the range from the melting temperature of the metal being welded to the boiling temperature and higher, for example, due to local heating of this surface by focused laser beam under hybrid welding conditions. In this temperature range, metal evaporation from the anode surface may occur both in the diffusive mode and in the convective one [9]. In the diffusive mode of evaporation, which is realized when the vapor pressure of the anode metal is less than the ambient plasma pressure, the evaporated metal particles diffuse into the arc plasma and it becomes multi-component (containing atoms and ions of the shielding/plasma-forming gas and of the anode metal). In the convective mode, the metal vapor pressure is greater than the ambient pressure. Hence, vapor expansion occurs from the anode surface, which displaces the shielding/plasma-forming gas, and the near-anode plasma becomes one-component (containing only atoms and ions of the anode metal).

For both considered evaporation modes, the influence of the anode metal evaporation on the welding arc plasma characteristics, as well as its effect on the metal being welded, is largely determined by the processes occurring in the anode boundary layer. Thus, studying the anode layer of the atmospheric pressure electric arc in the conditions of metal evaporation from the anode surface is an important step toward a deeper understanding of TIG/PTA and hybrid (TIG/PTA + laser) welding and toward a further improvement of the corresponding technologies.

Due to the small dimensions, high temperatures, rapid dynamics, and the difficulty of direct observation, experimental studies of anode phenomena are significantly complicated. Therefore, theoretical investigation and numerical modeling are effective tools for studying and analyzing the physical processes occurring in the anode boundary layer of welding arcs.

Note that the characteristic thickness of the anode layer L_a is usually much less than the size of the weld pool surface. Hence, the variations of plasma parameters inside the anode layer ($0 \le x \le L_a$) perpendicularly to the anode surface are much more rapid than the changes along this surface. It allows us to use the one-dimensional model of the anode boundary layer of arc plasma. We will consider the anode layer outside the region of spatial charge (sheath) ($0 \le x \le L_D$) (see Figure 1), which is formed near the surface of the anode and has a characteristic size of the order of Debye length $L_D \sim 10^{-7}$–10^{-8} m [10–11]. That is, in our model, the plasma of the anode layer is quasi-neutral, but ionization and thermally non-equilibrium (the temperature of electrons is not equal to that of heavy particles $T_e \neq T_h$). In addition, since the electron temperature of the near-anode plasma commonly does not exceed 12 kK [12], we will assume that it is singly ionized (containing only single-charged ions). In the convective mode of the anode metal evaporation, inside the anode boundary layer, the Knudsen layer for evaporated atoms can be distinguished $0 \le x \le L_K$, the thickness of which is of the order of the atom-atom mean free path, which for copper plasma of atmospheric pressure is $\sim 10^{-6}$ m [10]. In the arc column ($x \ge L_a$), the arc plasma is considered to be in ionization and thermal equilibrium.

MAIN EQUATIONS OF ANODE BOUNDARY LAYER MODEL

At first, we introduce main equations describing singly ionized multi-component (metal-gas) plasma, which is not in thermal and ionization equilibrium. The continuity equations are [13]

$$\nabla\left(n_\alpha u + J_\alpha\right) = \omega_\alpha, \tag{1}$$

where α = *e*, *im*, *ig*, *am*, *ag* (for electrons, metal and gas ions and atoms, respectively). Here $\nabla = \frac{d}{dx}$; n_α is the number density of species α; $u = \frac{1}{\rho}\sum_\alpha \rho_\alpha u_\alpha$ is the mass-average plasma velocity, where $\rho_\alpha = m_\alpha n_\alpha$ and u_α are the mass density and average velocity of the α-th plasma component; m_α is the mass of the corresponding particle; $\rho = \sum_\alpha \rho_\alpha$ is the mass density of whole plasma; $J_\alpha = n_\alpha \upsilon_\alpha$ is the diffusive flux density of α component, where υ_α is its diffusive velocity; ω_α is the term describing the variation of the number density of particles of α-kind due to ionization and recombination.

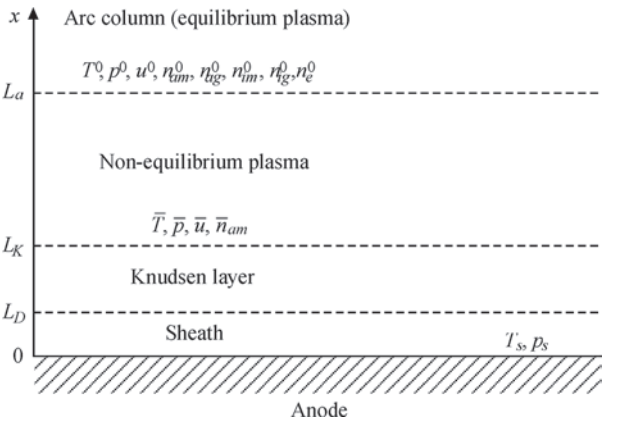

Figure 1. Scheme of the anode boundary layer

In high pressure discharges, the ionization is mainly driven by collisions between electrons and atoms and the dominant recombination mechanism is three-body recombination with an electron as the third body [14]. In this case, the production rates ω_α are written as

$$\begin{aligned} \omega_{im} &= -\omega_{am} = k_{im} n_e n_{am} - k_{rm} n_e^2 n_{im}, \\ \omega_{ig} &= -\omega_{ag} = k_{ig} n_e n_{ag} - k_{rg} n_e^2 n_{ig}, \\ \omega_e &= \omega_{im} + \omega_{ig}, \end{aligned} \tag{2}$$

where $k_{im,g}$ are the ionization rate constants of metal and gas atoms, respectively, and $k_{rm,g}$ are the corresponding recombination rate constants of ions.

The momentum equations are [13]

$$\begin{aligned} &\rho_\alpha u \nabla u + \nabla p_\alpha + z_\alpha e n_\alpha \nabla\varphi = \\ &= \sum_\beta \nu_{\alpha\beta} \mu_{\alpha\beta} n_\alpha n_\beta (\upsilon_\beta - \upsilon_\alpha) - R_\alpha^T. \end{aligned} \tag{3}$$

Here, $p_\alpha = n_\alpha k T_\alpha$ is the partial pressure of the α-th plasma component, where *k* is the Boltzmann constant and T_α is the temperature; z_α is the charge number ($z_e = -1$, $z_{im,ig} = 1$, $z_{am,ag} = 0$); *e* is the elementary charge; φ is the electrostatic potential; $\nu_{\alpha\beta}$ and $m_{\alpha\beta} = m_\alpha m_\beta/(m_\alpha + m_\beta)$ are the collision frequency and reduced mass of α and β species; R_α^T is thermal diffusion force related to the gradient of electron temperature:

$$R_\alpha^T = C_\alpha^{(e)} n_\alpha k \nabla T_e, \quad \sum C_\alpha^{(e)} n_\alpha = 0. \tag{4}$$

Note that the thermal diffusion effect due to the heavy particles' temperature gradient is neglected in equations (4) [15].

The energy equations are [13]

$$\begin{aligned} &\frac{3}{2} u \nabla p_\alpha + \frac{5}{2} p_\alpha \nabla u + m_\alpha J_\alpha u \nabla u + \nabla q_\alpha + z_\alpha e J_\alpha \nabla\varphi = \\ &= -\sum_\beta 3k \nu_{\alpha\beta} \frac{\mu_{\alpha\beta}}{m_\alpha + m_\beta} n_\alpha n_\beta (T_\alpha - T_\beta) - \delta_{\alpha e} w_e, \end{aligned} \tag{5}$$

where δ_{ae} is the Kronecker delta.

The heat fluxes q_α in equations (5) are assumed to be caused by the heat conduction and convection

$$q_\alpha = h_\alpha + \frac{5}{2} J_\alpha k T_\alpha . \qquad (6)$$

Here for heavy particles ($\alpha \neq e$) the conductive heat fluxes h_α can be defined without taking into account the effect inverse to the thermal diffusion [15].

$$h_\alpha = -\lambda_\alpha \nabla T_\alpha , \qquad (7)$$

where λ_α is the thermal conductivity coefficient of heavy particles species α. For electrons, both mechanisms (heat conduction and thermal diffusion) are taken into account, and the electron heat flux h_e is given by [15]:

$$h_e = -\lambda_e \nabla T_e + k T_e n_e \sum_\beta A_\beta^{(e)} (\upsilon_e - \upsilon_\beta), \qquad (8)$$

where λ_e is the electron thermal conductivity; $A_\beta^{(e)}$ are the kinetic coefficients.

The value w_e in equation (5) for electrons describes the energy losses of the electron component of the plasma due to atom ionization and radiation:

$$w_e = U_{im} \omega_{im} + U_{ig} \omega_{ig} + w_{rad} , \qquad (9)$$

where U_{im} and U_{ig} are the ionization potentials of the metal and gas atoms, respectively; w_{rad} is the power loss of electrons due to radiation.

The energy equations (5) can be written using the above assumption that the temperatures of all heavy particles are equal: $T_\alpha = T_h (\alpha \neq e)$, but differs from the electron temperature $T_e \neq T_h$ (two-temperature plasma model). In this case, the energy equation for electrons takes the form (neglecting the term with $m_e J_e u \nabla u$ [13] and taking into account the electron continuity equation):

$$\begin{aligned} &\left(n_e u + J_e\right)\frac{5}{2} k \nabla T_e - u \nabla (n_e k T_e) + \nabla h_e - e J_e \nabla \varphi = \\ &= -\kappa_{eh} n_e k (T_e - T_h) - \left(U_{im} + \frac{5}{2} k T_e\right)\omega_{im} - \\ &- \left(U_{ig} + \frac{5}{2} k T_e\right)\omega_{ig} - w_{rad} , \end{aligned} \qquad (10)$$

where

$$\kappa_{eh} = 3 \sum_{\beta \neq e} \nu_{e\beta} \frac{m_e}{m_\beta} n_\beta . \qquad (11)$$

Summing up equations (5) for plasma heavy particles, the energy equation for heavy particles can be written as:

$$\begin{aligned} &\sum_{\beta \neq e} \left\{ (n_\beta u + J_\beta)\frac{5}{2} k \nabla T_h - u \nabla (n_\beta k T_h) + \right. \\ &\left. + m_\beta J_\beta u \nabla u + z_\beta e J_\beta \nabla \varphi \right\} + \\ &+ \nabla h_h = \kappa_{eh} n_e k (T_e - T_h). \end{aligned} \qquad (12)$$

Here

$$h_h = -\lambda_h \nabla T_h , \qquad (13)$$

where $\lambda_h = \sum_{\beta \neq e} \lambda_\beta$ is the thermal conductivity of plasma heavy particles.

DIFFUSIVE EVAPORATION OF ANODE METAL

We consider a multi-component singly-ionized plasma of the anode boundary layer of an atmospheric pressure argon arc with a metal anode evaporating in the diffusive mode. The composition of such plasma is described by the number densities: n_e, n_{ig}, n_{im}, n_{ag}, n_{am}. The plasma in the anode layer (beyond the sheath) is quasi-neutral:

$$n_e = n_{ig} + n_{im} \qquad (14)$$

and it is assumed to be two-temperature ($T_e \neq T_h$).

Taking into account that atoms and ions of inert gas do not accumulate on the anode metal surface and assuming the total flux of heavy metallic particles (nuclei) from this surface G_m to be approximately equal to zero [16], we can write (relative to the anode surface):

$$\begin{aligned} (n_{ag} + n_{ig})u + J_{ag} + J_{ig} = 0, \\ (n_{am} + n_{im})u + J_{am} + J_{im} = G_m \approx 0. \end{aligned} \qquad (15)$$

In this case, up to terms of order $m_e/m_{g,m} \ll 1$, where $m_{g,m} = m_{ag,m} \approx m_{ig,m}$, the mass-average plasma velocity $u \approx 0$ and one can consider that plasma in the anode layer is stationary as a whole. As a result, equations (15) yield:

$$J_{ag} = -J_{ig} , \quad J_{am} = -J_{im} . \qquad (16)$$

From the expression for the electric current in the plasma $j_0 = e(J_{ig} + J_{im}) - eJ_e$ we have:

$$J_e = J_{ig} + J_{im} - j_0 / e . \qquad (17)$$

Thus, instead of five continuity equations (1) for diffusive fluxes J_e, J_{ig}, J_{im}, J_{ag}, J_{am}, only two equations can be solved for J_{ig} and J_{im}:

$$\nabla J_{ig} = \omega_{ig} , \quad \nabla J_{im} = \omega_{im} . \qquad (18)$$

Other diffusive fluxes are defined with Eqs (16) and (17).

Since the mass-averaged velocity of the near-anode plasma is assumed to be zero in the diffusive mode, then the pressure in the anode layer is constant (equal to atmospheric one). Using equation (14) we obtain

$$p_{atm} = n_{ag}kT_h + n_{ig}k(T_e + T_h) + \\ + n_{am}kT_h + n_{im}k(T_e + T_h). \quad (19)$$

Taking into account that $G_m \approx 0$, let us assume that the metal vapor in the anode layer is saturated and its partial pressure equals the metal vapor saturation pressure p_s at the corresponding surface temperature of the anode T_s, i.e. if $p_s(T_s) \le p_{atm}$, then $T_s \le T_B$, where T_B is the boiling temperature of the anode metal:

$$n_{am}kT_h + n_{im}k(T_e + T_h) = p_s(T_s). \quad (20)$$

Using Eqs (19) and (20), we can express n_{ag} and n_{am} in terms of n_{ig} and n_{im}, obtained as a result of solving equations (18):

$$n_{ag} = \frac{p_{atm} - p_s(T_s)}{kT_h} - n_{ig}\left(1 + \frac{T_e}{T_h}\right), \\ n_{am} = \frac{p_s(T_s)}{kT_h} - n_{im}\left(1 + \frac{T_e}{T_h}\right). \quad (21)$$

If $T_s = T_B$, then $p_s = p_{atm}$ and $n_{ag} = n_{ig} = 0$.

Further we consider the momentum equations (3) for plasma components (under the condition that $u = 0$). Adding the momentum equations for different charged plasma particles (electrons, metal ions and gas ions) to each other using Eqs (16), (17) and accounting for quasi-neutrality condition (14), we get from Eq. (3) that

$$-k(T_e + T_h)\left(\nabla n_{im} + \nabla n_{ig}\right) - \\ -\left(\tilde{C}_{im}^{(e)} n_{im} + \tilde{C}_{ig}^{(e)} n_{ig}\right)k\nabla T_e - \\ -\left(n_{im} + n_{ig}\right)k\nabla T_h + \\ + \alpha_{im}J_{im} + \alpha_{ig}J_{ig} + \alpha_j \frac{j_0}{e} = 0, \quad (22)$$

where

$$\alpha_{im} = -\nu_{eam}\mu_{em}(n_{im} + n_{am} + n_{ig}) - \\ -\nu_{eag}\mu_{eg}n_{ag} - \nu_{imam}\mu_{mm}(n_{im} + n_{am}) - \\ -\nu_{imag}\mu_{mg}n_{ag} - \nu_{igam}\mu_{gm}n_{ig}, \\ \alpha_{ig} = -\nu_{eam}\mu_{em}n_{am} - \nu_{eag}\mu_{eg}(n_{ig} + n_{ag} + n_{im}) - \\ -\nu_{igam}\mu_{gm}n_{am} - \nu_{igag}\mu_{gg}(n_{ig} + n_{ag}) - \nu_{imag}\mu_{mg}n_{im}, \quad (23) \\ \alpha_j = \nu_{eam}\mu_{em}n_{am} + \nu_{eag}\mu_{eg}n_{ag}, \\ \tilde{C}_{im}^{(e)} = 1 + C_e^{(e)} + C_{im}^{(e)}, \quad \tilde{C}_{ig}^{(e)} = 1 + C_e^{(e)} + C_{ig}^{(e)}.$$

As a second equation of the system, we will use the momentum equation (3) for metal atoms. Using the relations $\nabla(n_{ag}kT_h) = -\nabla[n_{ig}k(T_e + T_h)]$ and $\nabla(n_{am}kT_h) = -\nabla[n_{im}k(T_e + T_h)]$ following from Eqs (21), we get

$$k\left(T_e + T_h\right)\nabla n_{im} - \left(C_{am}^{(e)}\frac{p_s}{kT_h} - \tilde{C}_{am}^{(e)}n_{im}\right)k\nabla T_e + \\ + n_{im}k\nabla T_h + \beta_{im}J_{im} + \beta_{ig}J_{ig} + \beta_j\frac{j_0}{e} = 0, \quad (24)$$

where

$$\beta_{im} = \nu_{ame}\mu_{em}(n_{im} + n_{am} + n_{ig}) + \\ + \nu_{amim}\mu_{mm}(n_{im} + n_{am}) + \\ + \nu_{amig}\mu_{mg}n_{ig} + \nu_{amag}\mu_{mg}n_{ag}, \\ \beta_{ig} = \nu_{ame}\mu_{em}n_{am} + \\ + \nu_{amig}\mu_{mg}n_{am} - \nu_{amag}\mu_{mg}n_{am}, \quad (25) \\ \beta_j = -\nu_{eam}\mu_{em}n_{am}, \\ \tilde{C}_{am}^{(e)} = 1 + C_{am}^{(e)}\left(1 + T_e/T_h\right).$$

From Eqs (22) and (24) we can find the expressions for J_{im} and J_{ig} for the two continuity equations (18)

$$J_{im} = \frac{1}{\Delta}\{k(T_e + T_h)\times \\ \times\left[(\beta_{ig} + \alpha_{ig})\nabla n_{im} + \beta_{ig}\nabla n_{ig}\right] + \\ + \left[\beta_{ig}\left(\tilde{C}_{im}^{(e)}n_{im} + \tilde{C}_{ig}^{(e)}n_{ig}\right) - \right. \\ \left. -\alpha_{ig}\left(C_{am}^{(e)}\frac{p_s}{kT_h} - \tilde{C}_{am}^{(e)}n_{im}\right)\right]k\nabla T_e + \quad (26) \\ + \left[(\beta_{ig} + \alpha_{ig})n_{im} + \beta_{ig}n_{ig}\right]k\nabla T_h - \\ -(\beta_{ig}\alpha_j - \alpha_{ig}\beta_j)\frac{j_0}{e}\Big\};$$

$$J_{ig} = -\frac{1}{\Delta}\{k(T_e + T_h)\times \\ \times\left[\left(\beta_{im} + \alpha_{im}\right)\nabla n_{im} + \beta_{im}\nabla n_{ig}\right] + \\ + \left[\beta_{im}\left(\tilde{C}_{im}^{(e)}n_{im} + \tilde{C}_{ig}^{(e)}n_{ig}\right) - \right. \\ \left. -\alpha_{im}\left(C_{am}^{(e)}\frac{p_s}{kT_h} - \tilde{C}_{am}^{(e)}n_{im}\right)\right]k\nabla T_e + \quad (27) \\ + \left[(\beta_{im} + \alpha_{im})n_{im} + \beta_{im}n_{ig}\right]k\nabla T_h - \\ -\left[\beta_{im}\alpha_j - \alpha_{im}\beta_j\right]\frac{j_0}{e}\Big\}.$$

Here

$$\Delta = \alpha_{im}\beta_{ig} - \alpha_{ig}\beta_{im}. \quad (28)$$

Using the momentum equation (3) for electrons, the expression for determining $\nabla\varphi$ can be written as:

$$\nabla\varphi = \frac{1}{en_e}\left\{kT_e\nabla n_e + \left(1 + C_e^{(e)}\right)n_e k\nabla T_e - \right.$$
$$\left. -\delta_{im}J_{im} - \delta_{ig}J_{ig} - \delta_j\frac{j_0}{e}\right\}, \quad (29)$$

where

$$\delta_{im} = \nu_{eim}\mu_{em}n_{ig} - \nu_{eam}\mu_{em}(n_{im} + n_{am} + n_{ig}) -$$
$$-\nu_{eig}\mu_{eg}n_{ig} - \nu_{eag}\mu_{eg}n_{ag},$$
$$\delta_{ig} = -\nu_{eim}\mu_{em}n_{im} - \nu_{eam}\mu_{em}n_{am} +$$
$$+\nu_{eig}\mu_{eg}n_{im} - \nu_{eag}\mu_{eg}(n_{ig} + n_{ag} + n_{im}), \quad (30)$$
$$\delta_j = \nu_{eim}\mu_{em}n_{im} + \nu_{eam}\mu_{em}n_{am} +$$
$$+\nu_{eig}\mu_{eg}n_{ig} + \nu_{eag}\mu_{eg}n_{ag}.$$

The energy equation for heavy particles, which follows from Eq. (12) with $u = 0$, is

$$\nabla h_h = -e\left(J_{im} + J_{ig}\right)\nabla\varphi + \kappa_{eh}n_e k(T_e - T_h). \quad (31)$$

The energy equation for electrons, which follows from Eq. (10) with $u = 0$, is

$$\nabla\left(\frac{5}{2}kT_eJ_e + h_e\right) = eJ_e\nabla\varphi - \kappa_{eh}n_e k(T_e - T_h) -$$
$$-U_{im}\omega_{im} - U_{ig}\omega_{ig} - w_{rad}, \quad (32)$$

where $J_e = (J_{ig} + J_{im}) - j_0/e$.

Further, we consider the boundary conditions for four Eqs (18), (31) and (32). At the boundary between the anode layer and arc column ($x = L_a$), plasma is assumed to be spatially homogeneous and in both thermal and ionization equilibrium at a temperature T^0 and pressure p_{atm}. The position of the boundary $x = L_a$ is determined from the conditions $\nabla T_e\big|_{L_a} = \nabla T_h\big|_{L_a} = 0$ and $\nabla n_{im}\big|_{L_a} = \nabla n_{ig}\big|_{L_a} = 0$. The boundary conditions for corresponding equations can be written as:

$$T_e\big|_{L_a} = T_h\big|_{L_a} = T^0, \quad (33)$$

$$n_{im}\big|_{L_a} = n_{im}^0, \quad n_{ig}\big|_{L_a} = n_{ig}^0, \quad (34)$$

where n_{im}^0, n_{ig}^0 are determined from the following system of equations consisting of two Saha equations, quasi-neutrality condition and Eqs (21) for equilibrium plasma

$$\frac{n_e^0 n_{im}^0}{n_{am}^0} = S_m(T^0), \quad \frac{n_e^0 n_{ig}^0}{n_{ag}^0} = S_g(T^0),$$
$$n_e^0 = n_{im}^0 + n_{ig}^0, \quad n_{am}^0 = \frac{p_s(T_s)}{kT^0} - 2n_{im}^0, \quad (35)$$
$$n_{ag}^0 = \frac{p_{atm} - p_s(T_s)}{kT^0} - 2n_{ig}^0.$$

Here

$$S_\alpha(T^0) = \left(\frac{2\pi m_e kT^0}{h^2}\right)^{3/2}\frac{2\theta_{i\alpha}}{\theta_{a\alpha}}\exp\left(-\frac{eU_{i\alpha}}{kT^0}\right), \quad (36)$$

where h is the Planck constant; $\theta_{i\alpha} = (2L_{i\alpha} + 1)(2S_{i\alpha} + 1)$ and $\theta_{a\alpha} = (2L_{a\alpha} + 1)(2S_{a\alpha} + 1)$ are the partition functions (statistical weights) of the ion and the atom; $L_{i\alpha,a\alpha}$ and $S_{i\alpha,a\alpha}$ denote the total orbital and spin quantum number, respectively.

The system of equations (35) is a system of nonlinear algebraic equations for five unknowns n_e^0, n_{im}^0, n_{ig}^0, n_{am}^0, n_{ag}^0. The equation for determining T^0 can be written as follows. Since the plasma for $x \geq L_a$ is equilibrium and homogeneous, the energy equations (31) and (32) take the form:

$$-e(J_{im} + J_{ig})\nabla\varphi + \kappa_{eh}n_e k(T_e - T_h) = 0,$$
$$eJ_e\nabla\varphi - \kappa_{eh}n_e k(T_e - T_h) - w_{\text{rad}} = 0. \quad (37)$$

Adding these equations to each other, and accounting for the facts that $e(J_{im} + J_{ig} - J_e) = j_0$ and $j_0 = -\sigma_0\nabla\varphi$, we obtain

$$\frac{j_0^2}{\sigma_0(T^0)} = w_{\text{rad}}(T^0), \quad (38)$$

where $\sigma_0(T_0)$, $w_{rad}(T^0)$ are the electrical conductivity and the power loss due to radiation for a two-component plasma at atmospheric pressure and equilibrium temperature T^0.

In a homogeneous plasma Eqs (26), (27) and (29) take the form

$$J_{im} = -\frac{1}{\Delta}\left[\beta_{ig}\alpha_j - \alpha_{ig}\beta_j\right]\frac{j_0}{e},$$
$$J_{ig} = \frac{1}{\Delta}\left[\beta_{im}\alpha_j - \alpha_{im}\beta_j\right]\frac{j_0}{e}, \quad (39)$$
$$\nabla\varphi = -\frac{1}{en_e}\left[\delta_{im}J_{im} + \delta_{ig}J_{ig} + \delta_j\frac{j_0}{e}\right].$$

It follows (using $j_0 = -\sigma_0\nabla\varphi$):

$$\sigma_0 = \frac{w_1}{-w_2 + w_3 + w_4}, \quad (40)$$

where $w_1 = e^2n_e^0(\alpha_{im}\beta_{ig} - \alpha_{ig}\beta_{im})$; $w_2 = \delta_{im}(\beta_{ig}\alpha_j - \alpha_{ig}\beta_j)$; $w_3 = \delta_{ig}(\beta_{im}\alpha_j - \alpha_{im}\beta_j)$; $w_4 = \delta_j(\alpha_{im}\beta_{ig} - \alpha_{ig}\beta_{im})$.

Let us now consider the boundary conditions at $x = L_D$, i.e., at the boundary between the quasi-neutral plasma and the space-charge sheath, which at the atmospheric pressure of the near-anode plasma can be considered as collisionless both for electrons and ions [17]. Since the plasma is assumed to be station-

ary near the anode surface ($u = 0$) the temperature of the heavy particles is taken to be equal to the anode surface temperature

$$T_h\big|_{L_D} = T_s. \tag{41}$$

And the boundary condition for the electron temperature at the sheath edge can be written in the form [18]:

$$\left(h_e + \frac{5}{2}kT_eJ_e\right)\Big|_{L_D} = \left(2kT_e + e\varphi_{sh}\right)J_e\big|_{L_D}, \tag{42}$$

where h_e is defined by Eq. (8); φ_{sh} is the plasma potential at the boundary between the quasi-neutral plasma and the space-charge sheath (electric potential of the anode surface is assumed to be equal to zero). The electron diffusive flux density at this boundary is:

$$J_e\big|_{L_D} = -\frac{n_e\upsilon_{Te}}{4}\exp\left(-\frac{e\varphi_{sh}}{kT_e}\right), \quad \upsilon_{Te} = \sqrt{\frac{8kT_e}{\pi m_e}}. \tag{43}$$

Since the sheath is assumed to be collisionless for ions, then ion drift velocities at the boundary $x = L_D$ can be defined as [19, p. 183]:

$$u_{im}\big|_{L_D} = -\upsilon_{Bm}, \quad u_{ig}\big|_{L_D} = -\upsilon_{Bg}, \tag{44}$$

where

$$\upsilon_{Bm} = \sqrt{\frac{k(T_e+T_h)}{m_{im}}}, \quad \upsilon_{Bg} = \sqrt{\frac{k(T_e+T_h)}{m_{ig}}} \tag{45}$$

are the Bohm velocities for metal and gas ions. Thus,

$$J_{im}\big|_{L_D} = -n_{im}\upsilon_{Bm}, \quad J_{ig}\big|_{L_D} = -n_{ig}\upsilon_{Bg}. \tag{46}$$

Hence, Eqs (44)–(46) completely define the boundary conditions at $x = L_D$ for differential equations (18).

Using the condition $j_0 = e(J_{ig} + J_{im}) - eJ_e$ and Eqs (43), (46) we can find

$$\varphi_{sh} = -\frac{kT_e}{e}\ln\frac{4}{\upsilon_{Te}}\left(\frac{j_0}{en_e} + \frac{n_{im}\upsilon_{Bm} + n_{ig}\upsilon_{Bg}}{n_e}\right). \tag{47}$$

It should be noted here that the values of n_e, n_{im}, n_{ig}, T_e, T_h in expressions (43)–(47) are taken at $x = L_D$.

The numerical solution of the system of equations (18), (31) and (32) together with the corresponding boundary conditions allows us to determine the following characteristics of the plasma at the anode layer boundary with the space-charge sheath: n_{im}, n_{ig}, T_e, T_h, as well as the gradients of these quantities at this boundary. The quasi-neutrality condition (14) and relations (21) allow us to find n_e, n_{am} and n_{ag}, while relations (43)–(47) yield the values of J_{im}, J_{ig}, J_e, φ_{sh} at the sheath edge.

This enables computation of the heat flux introduced by the arc into the anode metal, taking into account its evaporation in the diffusive mode. This heat flux can be represented as:

$$q_a = \sum_{k=1}^{6} q_{ak}, \quad (q_{ak} > 0), \tag{48}$$

where

$$q_{a1} = \lambda_e\nabla T_e\big|_{L_D}, \qquad q_{a2} = \lambda_h\nabla T_h\big|_{L_D} \tag{49}$$

are the heat fluxes caused by heat conduction of electrons and heavy particles;

$$q_{a3} = -\left[\left(\frac{5}{2}kT_e - e\varphi_{sh}\right)J_e\big|_{L_D} + kT_e\sum_{\beta\neq e}A_\beta^{(e)}\left(J_e\big|_{L_D} - \frac{n_e}{n_\beta}J_\beta\big|_{L_D}\right)\right] \tag{50}$$

is the electron heat flux caused by convection, where the term $e\varphi_{sh}J_e\big|_{L_D}$ in the right-hand side of the expression (50) describes electron energy loss in the sheath electric field;

$$q_{a4} = -\left[\left(\frac{m_m\upsilon_{Bm}^2}{2} + e\varphi_{sh}\right)J_{im}\big|_{L_D} + \left(\frac{m_g\upsilon_{Bg}^2}{2} + e\varphi_{sh}\right)J_{ig}\big|_{L_D}\right] \tag{51}$$

is the heat flux caused by initial kinetic energy of ions on the sheath edge and their additional acceleration in the electric field of the sheath;

$$q_{a5} = -\left(U_{im}J_{im}\big|_{L_D} + U_{ig}J_{ig}\big|_{L_D}\right), \quad q_{a6} = \frac{j_0}{e}A_f \tag{52}$$

are the heat fluxes caused by the recombination of ions and absorption of electrons at the anode surface, where A_f is the electron work function of the anode metal. Since $J_e\big|_{L_D}$, $J_{im}\big|_{L_D}$, $J_{ig}\big|_{L_D}$ are negative, the minus sign was added in the expressions for q_{a3}, q_{a4}, q_{a5} to ensure that these heat flux components are positive.

CONVECTIVE MODE OF ANODE METAL EVAPORATION

Under the conditions of convective evaporation of an anode metal, the plasma in the anode boundary layer is one-component (contains only metal ions and atoms) and moves at a mass-average velocity u from the surface of the anode. In this case, the quasi-neutrality condition takes the form

$$n_e = n_{im}, \tag{53}$$

Taking into account that $m_eJ_e + m_m(J_{im} + J_{am}) = 0$ [13], up to terms of order $m_e/m_m << 1$ we have

$$J_{im} + J_{am} \approx 0. \tag{54}$$

Then the energy equations for heavy particles (12) and (10) electrons yield

$$\begin{aligned}\left(n_{im}+n_{am}\right)u\nabla\frac{5}{2}kT_h - u\nabla\left[\left(n_{im}+n_{am}\right)kT_h\right] = \\ = -\nabla h_h - eJ_{im}\nabla\varphi + \kappa_{eh}n_{im}k\left(T_e - T_h\right),\end{aligned} \tag{55}$$

$$\begin{aligned}\left(n_{im}u + J_e\right)\nabla\frac{5}{2}kT_e - u\nabla\left(n_{im}kT_e\right) = \\ = -\nabla h_e + eJ_e\nabla\varphi - \kappa_{eh}n_{im}k\left(T_e - T_h\right) - \\ -\left(U_{im} + \frac{5}{2}kT_e\right)\omega_{im} - w_{rad},\end{aligned} \tag{56}$$

where $J_e = J_{im} - j_0/e$.

In the convective mode of the anode metal evaporation we have to solve only one of the continuity equations (1), namely for metal ions

$$\nabla\left(n_{im}u + J_{im}\right) = \omega_{im} = k_{im}n_{im}n_{am} - k_{rm}n_{im}^3. \tag{57}$$

The expression for ion flux density and the expression for determining the electrical potential of a one-component plasma take the form [20]

$$\begin{aligned}J_{im} = \frac{1}{\gamma_e + \gamma_i}\times \\ \times\left\{-k\left(T_e + T_h\right)\frac{n_{am}}{n_{im}+n_{am}}\nabla n_{im} + kT_h\frac{n_{im}}{n_{im}+n_{am}}\nabla n_{am} - \right. \\ \left. -\left(\frac{n_{am}}{n_{im}+n_{am}} + C_e^{(e)} + C_i^{(e)}\right)n_{im}k\nabla T_e + \left(\zeta_e + \zeta_i\right)\frac{j_0}{e}\right\},\end{aligned} \tag{58}$$

$$\begin{aligned}\nabla\varphi = \frac{1}{n_{im}e(\gamma_i + \gamma_e)}\left\{\left[\left(\gamma_e\frac{n_{im}}{n_{im}+n_{am}} + \gamma_i\right)kT_e - \right.\right. \\ \left. -\gamma_e\frac{n_{am}}{n_{im}+n_{am}}kT_h\right]\nabla n_{im} + \gamma_e\frac{n_{im}}{n_{im}+n_{am}}kT_h\nabla n_{am} + \\ +\left[\gamma_e\left(\frac{n_{im}}{n_{im}+n_{am}} - C_i^{(e)}\right) + \gamma_e\left(1 + C_e^{(e)}\right)\right]\times \\ \left.\times n_{im}k\nabla T_e + \left(\gamma_e\zeta_i - \gamma_i\zeta_e\right)\frac{j_0}{e}\right\},\end{aligned} \tag{59}$$

where

$$\begin{aligned}\gamma_e = \nu_{eam}\mu_{em}\left(n_{im}+n_{am}\right), \\ \gamma_i = \nu_{imam}\mu_{mm}\left(n_{im}+n_{am}\right), \\ \zeta_e = \nu_{eim}\mu_{em}n_{im} + \nu_{eam}\mu_{em}n_{am}, \\ \zeta_i = -\nu_{eim}\mu_{em}n_{im}.\end{aligned} \tag{60}$$

Thus, Eqs (55), (56) and (57) present a system of three differential equations of the second order with respect to three unknown functions $T_h(x)$, $T_e(x)$ and $n_{im}(x)$. If we put in these equations $u = 0$, then they become equations for non-convective one-component plasma, which can be found in [10]. The system of Eqs (55), (56) and (57) also includes the parameters $n_{am}(x)$ and $u(x)$, which can be found from the conservation equations for the total particle flux and momentum flux

$$\begin{aligned}\rho(x)u(x) = \text{const} = C_1, \\ p(x) + \rho(x)u(x)^2 = \text{const} = C_2,\end{aligned} \tag{61}$$

where $\rho(x) = m_m(n_{im} + n_{am})$ is the density of the plasma (here it is taken into account that $m_e << m_m$, $m_m = m_{am} \approx m_{im}$), $p(x) = n_{im}k(T_e + T_h) + n_{am}kT_h$ is the pressure.

Further, we will formulate the boundary conditions for a system of differential equations (55), (56) and (57). First, we will consider the boundary conditions at the boundary of the anode layer with the arc column ($x = L_a$), where plasma is considered to be both in ionization and thermal equilibrium ($T^0 = T_e = T_h$), as well as homogeneous.

According to Ref. [9], we will assume that pressure p^0 and velocity u^0 are related by the Rankine–Hugoniot conditions for a shock wave that moves through an external unperturbed gas under conditions of convective evaporation

$$u^0 = \frac{p^0 - p_{atm}}{\sqrt{\frac{\rho_{ext}}{2}\left[p^0(\gamma+1) + p_{atm}(\gamma-1)\right]}}, \tag{62}$$

where p_{atm} is the atmospheric pressure (pressure in the external gas — argon); ρ_{ext} is the density of the external gas for $p = p_{atm}$ and $T_{ext} = 300$ K, $\gamma = 5/3$ is the adiabatic index for a monatomic gas.

To find the composition of plasma at $x = L_a$, we can use the system of equations consisting of Saha equation while taking into account the quasi-neutrality condition, and the partial pressures law for equilibrium plasma

$$\frac{\left(n_{im}^0\right)^2}{n_{am}^0} = S_m(T^0), \quad n_{am}^0 = \frac{p^0}{kT^0} - 2n_{im}^0. \tag{63}$$

The equation for T^0 is Eq. (38)

$$\frac{j_0^2}{\sigma(T^0, p^0)} = w_{rad}(T^0, p^0), \tag{64}$$

where

$$\sigma(T^0, p^0) = e^2 n_i^0\frac{\gamma_e + \gamma_i}{\gamma_i\zeta_e - \gamma_e\zeta_i}. \tag{65}$$

Thus, the plasma parameters n_{am}^0, n_{im}^0, T^0, p^0, u^0 at the boundary $x = L_a$ are determined from the equations (62), (63) and (64), which must be supplemented by

one of the equations (61). Therefore, it is necessary to define one of the constants C_1, C_2.

Next, we need to find the boundary conditions at the other boundary of the anode layer, namely at the boundary with the spatial charge layer $x = L_D$. At low velocity of convective motion of the metallic plasma from the anode surface, compared to the speed of sound, the parameters of the plasma atomic component (density, velocity and temperature) almost do not change within the Knudsen layer [21, 22], so these parameters can be determined for $x = L_K$. The values at this boundary are marked by a dash on top. Since the plasma here is weakly ionized $\overline{n}_{im} \ll \overline{n}_{am}$ [11], ions and electrons do not affect the formation of the Knudsen layer for atoms and the approach to its description proposed in the [9] can be used.

$$\frac{\overline{n}_{am}}{n_s} = \sqrt{\frac{T_s}{\overline{T}_h}}\left[\left(\xi^2 + \frac{1}{2}\right)e^{\xi^2}\,\mathrm{erfc}(\xi) - \frac{\xi}{\sqrt{\pi}}\right] + \\ + \frac{1}{2}\frac{T_s}{\overline{T}_h}\left[1 - \sqrt{\pi}\xi e^{\xi^2}\,\mathrm{erfc}(\xi)\right], \tag{66}$$

$$\frac{\overline{T}_h}{T_s} = \left[\sqrt{1 + \pi\frac{\xi^2}{64}} - \sqrt{\pi}\frac{\xi}{8}\right]^2, \tag{67}$$

where $\overline{n}_{am}$, $\overline{T}_h$ and $\overline{u} = \xi\sqrt{2k\overline{T}_h / m_m}$ are the number density, temperature and velocity of metal atoms at the boundary of the Knudsen layer; n_s is the number density of saturated vapor atoms at the surface temperature of the anode metal T_s.

The conservation equations (61) can be written as

$$\overline{n}_{am}\overline{u} = (n^0_{im} + n^0_{am})u^0, \\ \overline{n}_{am}k\overline{T}_h + m_m\overline{n}_{am}\overline{u}^2 = p^0 + m_m(n^0_{im} + n^0_{am})(u^0)^2. \tag{68}$$

Thus, to determine the six parameters, n^0_{am}, n^0_{im}, T^0, p^0, u^0, $\overline{u}$ we have six equations, respectively: (62), (63), (64), (68). The external parameters are j_0 and T_s. Thus, the boundary conditions for Eqs (55), (56) and (57) at $x = L_a$ have the form

$$T_h\big|_{L_a} = T_e\big|_{L_a} = T^0, \quad n_{im}\big|_{L_a} = n^0_{im}. \tag{69}$$

The temperature of heavy particles at $x = L_K$ is equals to

$$T_h\big|_{L_K} = \overline{T}_h. \tag{70}$$

As stated above, the condition (70) set at $x = L_K$, remains valid at $x = L_D$ and can be used as a boundary condition for Eq. (55).

The boundary condition for Eq. (56) at the boundary of the spatial charge (sheath) is determined by expressions (42) and (43).

Taking into account that in the convective mode of the anode metal evaporation $\overline{u} \neq 0$ and the near-anode plasma pressure $\overline{p} > p_{atm}$ (ion-atom collisions in the sheath become essential), the ion drift velocities at the boundary $x = L_D$ can be defined as [20]

$$u_{im}\big|_{L_D} = \overline{u} + \left.\frac{J_{im}}{n_{im}}\right|_{L_D} = -\overline{\upsilon}_{Bm}. \tag{71}$$

Here $\overline{\upsilon}_{Bm} = \dfrac{\upsilon_{Bm}}{\sqrt{1 + \pi L_D / 2l_{im}}}$ [23], where υ_{Bm} is the Bohm velocity for metal ions (45), l_{im} is the ion-atom mean free path in the sheath. And finally, the boundary condition for Eq. (57) is given by

$$J_{im}\big|_{L_D} = -n_{im}(\overline{u} + \overline{\upsilon}_{Bm}). \tag{72}$$

The value of the potential at the sheath edge takes the form

$$\varphi_{sh} = -\frac{kT_e}{e}\ln\frac{4}{\upsilon_{Te}}\left(\frac{j_0}{en_{im}} + \frac{\upsilon_{Bm}}{\sqrt{1 + \pi L_D / 2\lambda_{im}}} + \overline{u}\right). \tag{73}$$

The numerical solution of the system of equations (55)–(57) together with the corresponding boundary conditions allows determining the heat flux to the anode, which is evaporated in the convective mode. This heat flux can be represented as (48), where q_{a1}, q_{a2}, q_{a3},q_{a6} are given by (49), (50), (52) and

$$q_{a4} = -\left(\frac{m_m\overline{\upsilon}^2_{Bm}}{2} + e\varphi_{sh}\right)J_{im}\big|_{L_D}, \\ q_{a5} = -U_{im}\,J_{im}\big|_{L_D}. \tag{74}$$

Under the conditions of convective evaporation of the anode metal in the energy balance of the anode surface the energy losses of this surface due to evaporation should be taken into account

$$q_{ev} = -\overline{n}_{am}\overline{u}\lambda, \tag{75}$$

where λ is the work function of metal atoms (heat of vaporization per atom).

PLASMA PARAMETERS AT THE ANODE LAYER BOUNDARIES

In this section, some values of plasma parameters, as a function of T_s, $T^0(j_0)$, will be calculated for the three variants of the anode metal: iron, copper and aluminum, the outer (shielding/plasma-forming) gas being argon. The transition from the diffusive to the convective evaporation mode will also be considered.

As mentioned above, the transition from the diffusive to the convective evaporation mode of the anode metal is determined by the surface temperature of the

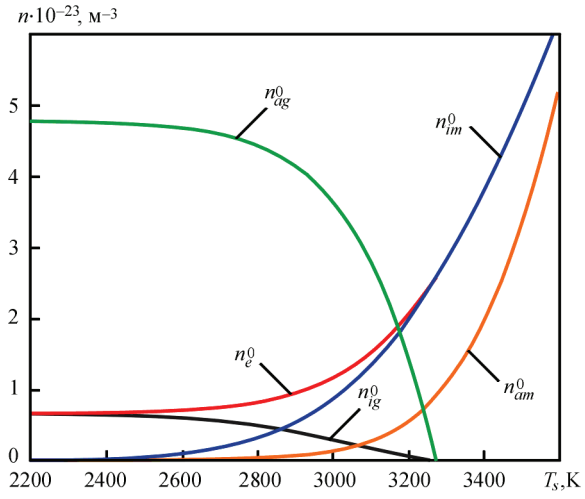

Figure 2. Number density of gas (Ar) atoms n_{ag}^0 (green line) and ions n_{ig}^0 (black line), electrons n_e^0 (red line), iron ions n_{im}^0 (blue line) and atoms n_{am}^0 (orange line) at the anode boundary layer edge vs. the temperature of the anode surface T_s for T^0 = 12 kK

anode T_s and the ambient gas pressure p_{ext}. For external pressure equal to the atmospheric one ($p_{ext} = p_{atm}$), the diffusive evaporation mode is realized for $T_s \le T_b$, and convective mode is realized for $T_s > T_b$, where T_b is the boiling point of the anode metal.

In the diffusive mode, the plasma of the anode boundary layer is multicomponent; in addition to particles of shielding/plasma-forming gas, it contains particles of the anode metal. The parameters of this multicomponent equilibrium plasma are defined by Eqs (35). The pressure of saturated vapor p_s, which enters the Eqs (35) is given by the Clapeyron–Clausius law

$$p_s = p_{atm} \exp\left[\frac{\lambda}{k}\left(\frac{1}{T_b} - \frac{1}{T_s}\right)\right]. \qquad (76)$$

Thus, we have a system of five equations (35) for five unknowns $n_{am}^0, n_{ag}^0, n_{im}^0, n_{ig}^0, n_e^0$.

For the convective evaporation mode, the equations for determining the parameters of the plasma at the boundary between the anode layer and the arc column are (62), (63), (64) and (65). Note, that the temperature of the plasma at this boundary T^0 is uniquely determined by the current density j_0 through equations (38) or (64), thus, T^0 can be used as the external parameter in subsequent calculations.

Calculations were performed for the atmospheric pressure argon arc with an iron, copper and aluminum anode under the condition of diffusive and convective evaporation of the metal from the anode surface. The boiling point of Fe was taken equal to T_b = 3273 K, the heat of vaporization was taken as 354 kJ/mol [24]. The first ionization potential is equal to 7.9025 eV, the ground states of the iron atom and ion are $^5D_4$ and $^6D_{9/2}$ [25], then θ_a = 25 and θ_i = 30. For Cu anode, T_b = 2868 K, the heat of vaporization is 305 kJ/mol, the first ionization potential is 7.726 eV [26]. The ground states of the copper atom and ion are: $^2S_{1/2}$ and $^1S_0$ [25] (θ_a = 2 and θ_i = 1). For Al we have T_b = 2743 K, the heat of vaporization is 284 kJ/mol, the first ionization potential is 5.986 eV [26]. The ground states of the aluminum atom and ion are $^2D_{1/2}$ and $^1S_0$ [25] (θ_a = 9 and θ_i = 1).

Figure 2 shows the results of calculations for the iron anode. As can be seen from this figure, when the surface temperature reaches the boiling point of iron T_b, the number density of gas (Ar) atoms and ions decreases to zero and the plasma becomes one-component (contains only Fe atoms and ions), i.e. there is a transition to the convective evaporation mode. In the diffusive mode, both gas and metal ions are present in the plasma, and in the convective mode only metal ions are present, the number density of which is equal to the number density of electrons (the blue and red

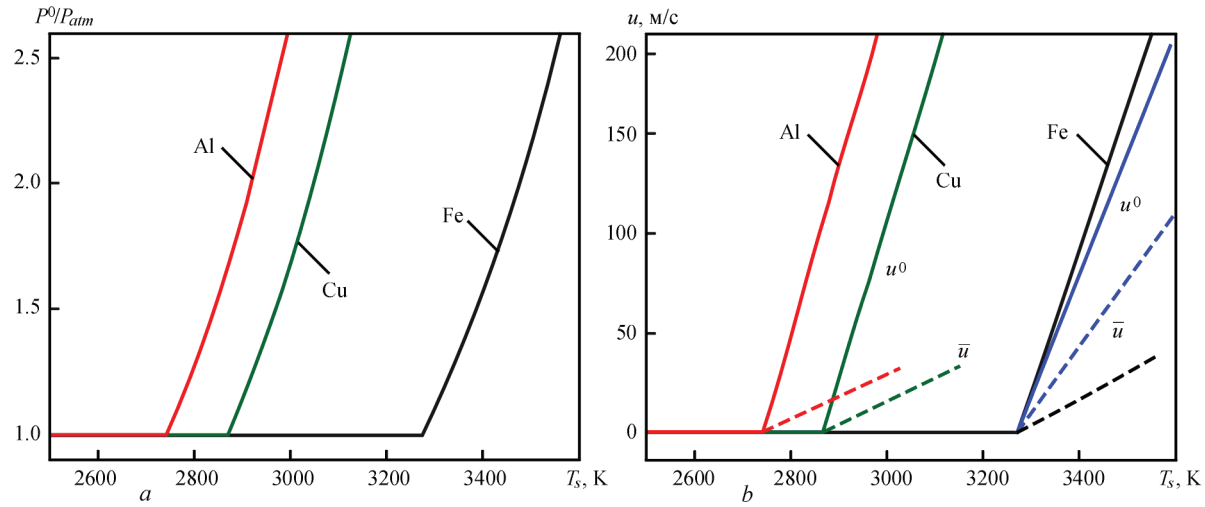

Figure 3. Plasma pressure p^0/p_{atm} (*a*), metal vapor velocity u^0 at the boundary between the anode layer and the arc column (solid lines) and velocity $\bar{u}$ at the boundary of the Knudsen layer (dashed lines) (*b*) vs. the surface temperature of the anode T_s for various anode metals: iron (black lines), copper (green lines) and aluminum (red lines), T^0 = 12 kK. Blue lines correspond to the iron anode and T^0 = 6 kK

lines in Figure 2 coincide for $T_s > T_b$). As the surface temperature increases, the number density of metal atoms in the plasma becomes higher. For other anode metals, the qualitative behavior of number density dependencies on surface temperature remains the same.

In the convective mode (see Figure 3), the velocity of the metal vapor u^0 becomes greater than zero and the pressure in the arc plasma p^0 becomes higher than the atmospheric pressure; both of these values increase with increasing T_s. The velocity of the metal vapor at the boundary of the Knudsen layer $\overline{a}$ is less than u^0. The velocities u^0 and $\overline{u}$ depend on T_s linearly. As a result of the approximation, we get the following:

$$\text{(Fe, } T_b = 3.273 \text{ kK)}\ u^0(T^0, T_s) = a(T^0)(T_s\,[\text{kK}] - T_b),$$
$$a(T^0) = 514.2 + 17.15T^0\ [\text{kK}];$$
$$\overline{u}\ (T^0, T_s) = \overline{a}\ (T^0)(T_s\,[\text{kK}] - T_b),$$
$$\overline{a}\ (T^0) = 673 - 65.22T^0\ [\text{kK}] + 1.66(T^0\ [\text{kK}])^2;$$
$$\text{(Cu, } T_b = 2.868 \text{ kK)}\ u^0(T^0, T_s) = a(T^0)(T_s\,[\text{kK}] - T_b),$$
$$a(T^0) = 567.7 + 20.52T^0\ [\text{kK}];$$
$$\overline{u}\ (T^0, T_s) = \overline{a}\ (T^0)(T_s\,[\text{kK}] - T_b),$$
$$\overline{a}\ (T^0) = 714.3 - 77.31T^0\ [\text{kK}] + 2.28(T^0\ [\text{kK}])^2;$$
$$\text{(Al, } T_b = 2.743 \text{ kK)}\ u^0(T^0, T_s) = a(T^0)(T_s\,[\text{kK}] - T_b),$$
$$a(T^0) = 577.7 + 38.18T^0\ [\text{kK}] - 1.28(T^0\ [\text{kK}])^2;$$
$$\overline{u}\ (T^0, T_s) = \overline{a}\ (T^0)(T_s\,[\text{kK}] - T_b),$$
$$\overline{a}\ (T^0) = 859.8 - 106.9T^0\ [\text{kK}] + 3.75(T^0\ [\text{kK}])^2.$$

As can be seen from the approximation formulas, as well as from the comparison of the black (Fe, T^0 = 12 kK) and blue (Fe, T^0 = 6 kK) lines in Figure 3, *b*, with increasing T^0, $\overline{u}$ decreases, and u^0 on the contrary increases. The calculations also showed that in the selected range of T_s, $\overline{p} \approx p^0$.

RESULTS AND CONCLUSIONS

A one-dimensional model of the anode boundary layer in welding arcs under TIG/PTA, and hybrid (TIG/PTA + laser) welding conditions (atmospheric pressure inert gas electric arc with refractory cathode and evaporating anode) is formulated for two modes of the anode metal evaporation: the diffusive and convective mode. The model consists of a system of the differential and algebraic equations for calculating the spatial distributions of the number densities of electrons, ions and atoms, their diffusive flux densities, electron temperature, heavy particle (atoms and ions) temperature and electric potential in the plasma of the anode layer. The model also allows calculating the heat flux introduced by the arc into the anode. The boundary conditions for the differential equations of this model at the boundaries of the anode layer with the arc column and the space-charge sheath are determined. An approach is proposed for calculating the near-anode plasma parameters at these boundaries, both in the case of the diffusive evaporation mode of the anode metal and in the convective mode.

For three different anode metals (Fe, Cu, Al), the dependencies of the number densities of plasma particles, pressure and velocity of ionized metal vapor at the anode layer boundaries on the surface temperature of the anode T_s (in the range of 2200 K $\le T_s \le T_b$ + 300 K) are calculated for both diffusive and convective modes of evaporation at fixed value of the arc column plasma temperature T^0 (in the range of 6 kK $\le T^0 \le$ 12 kK).

For the atmospheric pressure argon arc with a refractory cathode and evaporating anode under the condition of its diffusive evaporation ($T_s \le T_b$) the near-anode plasma is multicomponent (Ar + Me). Its mass-average velocity is negligible (up to the diffusive flux of the metal heavy particles G_m [16]). The plasma pressure is equal to the atmospheric pressure, and as the anode surface temperature increases, the number densities of metal atoms and ions in the near-anode plasma also increase. It should be noted that, as it follows from Eq. (76), at $T_s \le T_b \Big/ \left(1 + 4.605\frac{kT_b}{\lambda}\right)$ the fraction of the metal particles in the near-anode plasma is less than 1 % and it can be considered as one-component argon plasma.

It is shown that in the convective mode of the anode metal evaporation ($T_s > T_b$) the velocities u^0 and $-$ linearly depend on T_s, and also depend on the temperature of the arc column T^0. The pressure at the boundary of the Knudsen layer $\overline{p}$ is almost equal to the pressure at the boundary with the arc column p^0 under the considered conditions.

ACKNOWLEDGMENT

The work was funded by the German Research Foundation (DFG) under grant RE2755/78-1. The authors would like to express sincere gratitude for the sponsorship and the support.

REFERENCES

1. Murphy, A.B. (2010) The effects of metal vapour in arc welding. *J. of Physics D: Applied Physics*, **43**, 434001, 91–104. DOI: https://doi.org/10.1088/0022-3727/43/43/434001
2. Schnick, M., Fuessel, U., Hertel, M. et al. (2010) Modelling of gas-metal arc welding taking into account metal vapour. *J. of Physics D: Applied Physics*, **43**, 434008. DOI: https://doi.org/10.1088/0022-3727/43/43/434008
3. Hertel, M., Trautmann, M., Jäckel, S., Füssel, U. (2017) The role of metal vapour in gas metal arc welding and methods of combined experimental and numerical process analysis. *Plasma Chemistry and Plasma Processing*, **37**, 531–547. DOI: https://doi.org/10.1007/s11090-017-9790-1
4. Cho, Y.T., Cho, W.I., Na, S.J. (2011) Numerical analysis of hybrid plasma generated by Nd:YAG laser and gas tungsten arc. *Optics & Laser Technology*, **43**, 711–720. https://doi.org/10.1016/j.optlastec.2010.09.013
5. Tanaka, M., Tsujimura, Y., Yamazaki, K. (2012) Dynamic behaviour of metal vapour in arc plasma during TIG welding.

Welding in the World, **56**, 30-36. DOI: https://doi.org/10.1007/BF03321142
6. Mougenot, J., Gonzalez, J.J., Freton, P., Masquère, M. (2013) Plasma-weld pool interaction in tungsten inert-gas configuration. *J. of Physics D: Applied Physics*, **46**, 135206. DOI: https://doi.org/10.1088/0022-3727/46/13/135206
7. Krivtsun, I., Demchenko, V., Krikent, I. et al. (2015) Distributed and integrated characteristics of the near-anode plasma of the welding arc in TIG and hybrid (TIG+CO_2-laser) welding. *Mathematical Modelling of Weld Phenomena*, **11**, 837–874.
8. Krivtsun, I.V. (2018) Anode processes in welding arcs. *The Paton Welding J*, **11–12**, 91—104. DOI: DOI: http://dx.doi.org/10.15407/tpwj2018.11–12.10
9. Knight, C.J. (1979) Theoretical modeling of rapid surface vaporization with back pressure. *AIAA J.*, **17**, 519–523. DOI: https://doi.org/10.2514/3.61164
10. Krivtsun, I.V., Momot, A.I., Denysenko, I.B. et al. (2024) Transport properties and kinetic coefficients of copper thermal plasmas. *Physics of Plasmas*, **31**, 083505. DOI: https://doi.org/10.1063/5.0216753
11. Krivtsun, I.V., Momot, A.I., Antoniv, D.V., Qin, B. (2023) Characteristics of atmospheric pressure Ar-plasma around a spherical particle: Numerical study. *Physics of Plasmas*, **30**, 043513. DOI: https://doi.org/10.1063/5.0141015
12. Heberlein, J., Mentel, J., Pfender, E. (2009) The anode region of electric arcs: a survey. *J. of Physics D: Applied Physics*, **43**, 023001. DOI: https://doi.org/10.1088/0022-3727/43/2/023001
13. Zhdanov, V.M. (2002) *Transport processes in multicomponent plasma*. CRC Press.
14. Almeida, N.A., Benilov, M.S., Naidis, G.V. (2008) Unified modelling of near-cathode plasma layers in high-pressure arc discharges. *J. of Physics D: Applied Physics* **41**, 245201. DOI: https://doi.org/10.1088/0022-3727/41/24/245201
15. Semenov, I.L., Krivtsun, I.V., Reisgen, U. (2016) Numerical study of the anode boundary layer in atmospheric pressure arc discharges. *J. of Physics D: Applied Physics*, **49**, 105204. DOI: https://doi.org/10.1088/0022-3727/49/10/105204
16. Krikent, I.V., Krivtsun, I.V., Demchenko, V.F. (2014) Simulation of electric arc with refractory cathode and evaporating anode, *The Paton Welding J.*, **9**, 17–24. DOI: https://doi.org/10.15407/tpwj2014.09.02
17. Benilov, M.S., Marotta, A. (1995) A model of the cathode region of atmospheric pressure arcs. *J. of Physics D: Applied Physics*, **28**, 1869. DOI: https://doi.org/10.1088/0022-3727/28/9/015
18. Gao, S., Momot, A., Krivtsun, I. et al. (2025) Interaction between a spherical particle and atmospheric pressure current-less argon plasma. *East European J. of Physics*, 388–395. DOI: https://doi.org/10.26565/2312-4334-2025-1-48
19. Lieberman, M.A., Lichtenberg, A.J. (1994) *Principles of plasma discharges and materials processing*. Wiley.
20. Krivtsun, I.V., Momot, A.I., Denysenko, I.B. (2025) Model of the anode layer of an electric arc with an evaporating anode, *Avtomatyche Zvaryuvannya*, **3**, 3–9.
21. Frezzotti, A. (2007) A numerical investigation of the steady evaporation of a polyatomic gas. *European J. of Mechanics-B/Fluids*, **26**, 93–104. DOI: https://doi.org/10.1016/j.euromechflu.2006.03.007
22. Bird, E., Liang, Z. (2019) Transport phenomena in the Knudsen layer near an evaporating surface. *Physical Review E*, **100**, 043108. DOI: https://doi.org/10.1103/PhysRevE.100.043108
23. Godyak, V.A., Sternberg, N. (2002) Smooth plasma-sheath transition in a hydrodynamic model. *IEEE Transact. on Plasma Sci.*, **18**, 159–168. DOI: https://doi.org/10.1109/27.45519
24. Zhang, Y., Evans, J.R., Yang, S. (2011) Corrected values for boiling points and enthalpies of vaporization of elements in handbooks. *J. of Chemical & Engineering Data*, **56**, 328–337. DOI: https://doi.org/10.1021/je1011086
25. Kramida, A., Ralchenko, Yu., Reader, J., NIST ASD Team (2024) *NIST Atomic Spectra Database* (ver. 5.12), Online. https://physics.nist.gov/asd National Institute of Standards and Technology, Gaithersburg, MD. DOI: https://doi.org/10.18434/T4W30F
26. Loock, H.P., Beaty, L.M., Simard, B. (1999) Reassessment of the first ionization potentials of copper, silver, and gold. *Physical Review A*, **59**, 873. https://doi.org/10.1103/PhysRevA.59.873

ORCID
I.V. Krivtsun: 0000-0001-9818-3383,
A.I. Momot: 0000-0001-8162-0161,
I.B. Denysenko: 0000-0001-7343-086X,
U. Reisgen: 0000-0003-4920-2351,
O. Mokrov: 0000-0002-9380-6905,
R. Sharma: 0000-0002-6976-4530

CONFLICT OF INTEREST
The Authors declare no conflict of interest

CORRESPONDING AUTHOR
A.I. Momot
E.O. Paton Electric Welding Institute of the NASU
11 Kazymyr Malevych Str., 03150, Kyiv, Ukraine.
E-mail: momot.andriy@gmail.com

SUGGESTED CITATION
I.V. Krivtsun, A.I. Momot, I.B. Denysenko, U. Reisgen, O. Mokrov, R. Sharma (2025) Model of the anode boundary layer in welding arcs. *The Paton Welding J.*, **8**, 44–54.
DOI: https://doi.org/10.37434/tpwj2025.08.05

JOURNAL HOME PAGE
https://patonpublishinghouse.com/eng/journals/tpwj

Received: 12.05.2025
Received in revised form: 17.06.2025
Accepted: 24.07.2025